

GeoFlink: A Framework for the Real-time Processing of Spatial Streams

Salman Ahmed Shaikh, Komal Mariam*, Hiroyuki Kitagawa†, Kyoung-Sook Kim
Artificial Intelligence Research Center

National Institute of Advanced Industrial Science and Technology (AIST)
2-4-7 Aomi, Koto-ku, Tokyo, Japan

*School of Electrical Engineering and Computer Science, National University of Sciences and Technology
H-12, Islamabad, Pakistan

†Center for Computational Sciences, University of Tsukuba
1-1-1 Tennodai, Tsukuba, Ibaraki, Japan

{shaikh.salman,ks.kim}@aist.go.jp, *kmariam.msee17seecs@seecs.edu.pk, †kitagawa@cs.tsukuba.ac.jp

Abstract—Apache Flink is an open-source system for the scalable processing of batch and streaming data. Flink does not natively support efficient processing of spatial data streams, which is the requirement of many applications dealing with spatial data. Besides Flink, other scalable spatial data processing platforms including GeoSpark, Spatial Hadoop, GeoMesa and Parallel Secondo do not support streaming workloads and can only handle static/batch workloads. Hence this work presents GeoFlink, which extends Apache Flink to support spatial data types, index and continuous queries. To enable efficient processing of continuous spatial queries and for the effective data distribution among the Flink cluster nodes, a grid-based index is introduced. The grid index enables the pruning of spatial objects which cannot be part of a spatial query result and thus can guarantee efficient query processing, similarly it helps in preserving spatial data proximity, hence resulting in effective data distribution. GeoFlink currently supports spatial range, spatial k NN and spatial join queries. An extensive experimental study on real spatial data streams show that GeoFlink achieves several orders of magnitude higher query performance than other ordinary distributed approaches.

Index Terms—

I. INTRODUCTION

With the increase in the use of GPS-enabled devices, spatial data is omnipresent. Such data includes people movement data, vehicles trajectory data, animals tracking data, geo-tagged social media data to name a few. Many applications require real-time processing of spatial data, for instance, to guide people to safety in a disaster. This entails real-time processing of billions of tuples per second. Existing spatial data processing frameworks for instance PostGIS [1] and QGIS [2] are not scalable to handle such huge data and throughput requirements, while scalable platforms like Apache Spark [3], Apache Flink [4], Apache Samza [5] and Apache Storm [6] do not natively support spatial data processing and randomly distribute incoming data to available nodes without considering its spatial data proximity, resulting in increased querying cost.

Beside these, there exist a few solutions to handle large scale spatial data, for instance Hadoop GIS [7], Spatial Hadoop

[8], GeoSpark [9], Parallel Secondo [10] and GeoMesa [11], however they are only suitable for static/batch processing and cannot handle real-time spatial streams. Hence this work presents GeoFlink, which extends Apache Flink to support distributed and scalable processing of spatial data streams. Namely, GeoFlink extends Apache Flink to support spatial data types, spatial index and spatial queries.

To enable the real-time processing of spatial data streams, a light weight grid-based index is introduced. Unlike static data, stream tuples arrive and expire at a high velocity and hence tree-based spatial indexes are not suitable for it owing to their high maintenance cost [12]. In fact the grid-based index used in this work is logical in the sense that it only assigns a grid ID to the incoming streaming tuples or moving objects and based on the grid ID the objects are processed, pruned and distributed across the cluster nodes. We do not physically store the objects in the data structure, hence no update is required as we receive an updated object location. Furthermore, given Flink’s key-based data distribution, the grid-based index is quite effective in distributing dynamic spatial data streams across the distributed cluster nodes by keeping in view the spatial data proximity as discussed in Section VII.

Many database operators are blocking, i.e., they require the entire input before an output can be generated. For example, the aggregation and join operators require processing of the entire dataset before outputting the correct result. Since the data streams are continuous and infinite, we can never see it entirely. Therefore windows are used to bound and execute different operations on data streams. Apache Flink [4] supports many different types of windows, which causes the continuous queries output to be generated periodically, i.e., hourly, daily, weekly, etc., or for some fixed number of tuples. Similarly, the GeoFlink operators i.e., spatial range, spatial k NN and spatial join queries, are also window-based. The grid-based GeoFlink queries are evaluated against the respective ordinary Apache Flink’s distributed queries. To summarize, the following key contributions are made in this paper:

- The core of GeoFlink, which extends Apache Flink to

- support spatial data types, index and continuous queries.
- Grid-based spatial data index for the efficient spatial queries' processing and effective data partitioning across the cluster nodes.
- Optimized grid-based spatial range, spatial k NN and spatial join queries.
- An extensive experimental study on real spatial data streams to show that GeoFlink achieves several orders of magnitude higher query performance than the ordinary distributed approaches.

The rest of the paper is organized as follows: Section II presents the related work. Section III briefly discusses the Flink programming model and its limitations. In Section IV the proposed GeoFlink architecture is presented. Section V presents the grid index used in GeoFlink. Sections VI and VII detail the Spatial Stream and the Spatial Queries layers of GeoFlink. In Section VIII detailed experimental study is presented while Section IX concludes our paper and highlights a few future directions.

II. RELATED WORK

Existing spatial data processing frameworks like ESRI ArcGIS [13], PostGIS [1] and QGIS [2] are built on relational DBMS and are therefore not scalable to handle huge data and throughput requirements. Authors in [14] extend SQL by integrating spatio-temporal data as abstract data types into already existing data models and present *STQL* (Spatio-temporal Query Language), which enables querying moving objects. The authors describe the moving objects as geometries changing continuously over time. The authors present a DBMS data model and query language capable of handling such time-dependent geometries. Their model focuses on moving points (cars, planes, animals, people) and moving regions (storms, people, temperature zones, high or low pressure areas).

Beside these, there exist a few solutions to handle large scale spatial data, for instance Hadoop GIS [7], Spatial Hadoop [8], GeoSpark [9], Parallel Secondo [10] and GeoMesa [11], however they are only suitable for static/batch processing and cannot handle real-time spatial streams. Among the above mentioned spatial data processing frameworks, GeoSpark is closest to our work. GeoSpark is a spatial data management and processing framework, which extends the core engine of Apache Spark and SparkSQL to support spatial data types, indexes and geometrical operations. However, it does not support continuous processing of spatio data streams [9] as we do.

Large-scale real-time computation in the order of millions and billions of tuples is only possible with the help of state-of-the-art distributed and horizontally scalable big data processing platforms like Apache Spark [3] and Apache Flink [4]. These distributed batch and streaming platforms are built to handle large throughputs and dynamically changing data, however, do not natively support spatial data processing and hence do not support spatial data types, spatial indexes and meaningful spatial data distribution (which takes into account the spatial proximity of data) across the cluster nodes.

A number of researchers, both from academia and industry, have put efforts to extend the above mentioned scalable platforms for the processing of spatial data. SpatialSpark [15] leverages Apache Sparks broadcast mechanism to provide partitions based on broadcast space. GeoSpark [9] processes spatial data by extending Sparks native Resilient Distributed Dataset (RDD) to create Spatial RDD (SRDD) along with a Spatial Query Processing layer on top of the Spark API to run spatial queries on these SRDDs. For efficient spatial query processing, GeoSpark creates a local spatial index (Grid, R-tree) per RDD partition rather than a single global index. For re-usability, the created index can be cached on main memory and can also be persisted on secondary storage for later use. However, the index once created cannot be updated, and must be recreated to reflect any change in the dataset due to the immutable nature of RDDs.

LocationSpark [16], GeoMesa [11] and Spark GIS [17] are a few other spatial data processing frameworks developed on top of Apache Spark. All these frameworks, like the GeoSpark, are scalable however can only handle static/batch datasets and do not support real-time stream processing as we do in GeoFlink.

To support real-time queries, Apache Spark introduces Spark Streaming that relies on micro-batches to address latency concerns and mimic streaming computations. Latency is inversely proportional to batch size however, the experimental evaluations in [18] show that as the batch size is decreased to very small to mimic the real-time streams, Apache Spark is prone to system crashes and exhibits lower fault tolerance. Furthermore, even with the micro-batching technique, Spark only approaches near real-time results at best, as data buffering latency still exists however miniscule.

Other distributed streaming platforms worth considering are Apache Samza [5] and Apache Storm [6]. Performance comparison by Fakrudeen et al. [18] reveal that both the Storm and Samza demonstrate a lower throughput and reliability than Apache Flink [4]. Indeed F. Zhang et al. [9] mentions that the architecture of their spatial querying framework could demonstrate a higher throughput if implemented on Apache Flink.

To support real-time processing of spatial data streams, Zhang et al. [19] extend Apache Storm. They proposed and implemented distributed spatial indexing for efficient continuous spatial query processing. The grid index in their work consists of a primary index (of the grid cells) and a secondary index (of the individual cell objects). The secondary index is tree-based and physically stores the moving objects and must be updated as the object moves or updated. In contrast, the grid index in GeoFlink is logical, in the sense that it only assigns a grid ID to the incoming streaming tuples or moving objects and based on the grid ID the objects are processed, pruned and distributed across the cluster nodes. We do not physically store the objects in any data structure, hence no update is required as we receive an updated object location. Hence enabling GeoFlink to achieve higher query throughput.

In light of the above discussed works, this paper presents GeoFlink, a distributed and scalable framework for real-time

processing of spatial data streams. To enable efficient spatial query processing and effective spatial data distribution across the cluster nodes, a light-weight logical grid-based index is proposed.

III. FLINK DATAFLOW PROGRAMMING MODEL AND ITS LIMITATIONS TO SUPPORT SPATIAL DATA

Apache Flink uses the following two data collections to represent data in a program: 1) DataSet: Represents a static and finite collection of tuples, 2) DataStream: Represents a continuous and infinite/unbounded collection of tuples. However, the DataSets used in Flink's DataSet API are also streams internally. A Flink program has 3 basic building blocks: 1) Source, 2) Transformations and 3) Sink. Conceptually a stream is a (potentially never-ending) flow of data records, and a transformation is an operation that takes one or more streams as input, and produces one or more output streams as a result. When executed, Flink programs are mapped to streaming dataflows, consisting of streams and transformation operators. Each dataflow starts with one or more sources and ends in one or more sinks. The dataflows resemble arbitrary Directed Acyclic Graphs (DAGs), however special forms of cycles are permitted via iteration constructs [20]. By its very definition dataflow processing offers lower latency with the price of lower fault tolerance. To address the need for fault tolerance, Flink provides distributed check-pointing and program resumption mechanism upon failure while maintaining its exactly once semantics. Thus, for real-time analytics use cases a natural choice is to use Apache Flink.

In a Flink's streaming program, one can refer to different notions of time: 1) Event Time is the time when an event was created. It is usually described by a timestamp in the events. 2) Ingestion Time is the time when an event enters the Flink dataflow at the source operator. 3) Processing Time is the local time at each operator that performs a time-based operation. Aggregates on streams (counts, sums, etc.), are scoped by windows, such as "count over the last 5 minutes", or "sum of the last 100 elements", since it is impossible to count all elements in a stream, because streams are in general infinite (unbounded). Windows can be time driven (example: every 30 seconds) or data driven (example: every 100 elements). One typically distinguishes different types of windows, such as tumbling windows (no overlap), sliding windows (with overlap), and session windows (punctuated by a gap of inactivity). When using windows, output is generated based on the complete window contents as the window moves.

Flink's DataStream API enables transformations like filter, map, reduce, keyby, aggregations, window, etc. on unbounded data streams of data and provides seamless connectivity with data sources and sinks like Apache Kafka (source/sink), Apache Cassandra (sink), etc. [20]. While many operations in a dataflow simply look at one individual event at a time, some operations remember information across multiple events (for example window operators). These operations are called stateful.

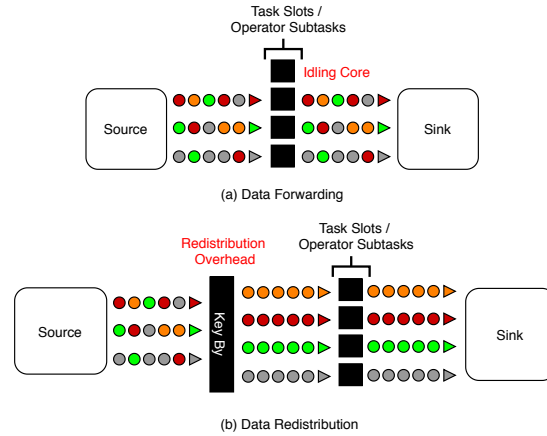


Fig. 1. Data forwarding vs. Data redistribution

Programs in Flink are inherently parallel and distributed. During execution, an operator is divided into one or more subtasks (operator instances) which are independent of one another and execute in different threads that may be on different machines or containers. The number of an operator's subtasks depends on the amount of its parallelism. A user can define the parallelism of each operator or set the maximum parallelism globally for all operators. Flink parallelism depends on the number of available task slots, where a good default number of task slots is equivalent to the number of CPU cores.

In Flink, keys are responsible for the data distribution across the task slots or operator instances. All the tuples with the same key are guaranteed to be processed by a single operator instance. In addition, many of Flink's core data transformations like join, groupBy, reduce and windowing require the data to be grouped on keys. Keying operations are enabled by the *keyBy* operator, which logically partitions stream tuples with respect to their keys. Intelligent key assignment ensures uniform data distribution among operator instances and hence leverages the performance offered by parallelism.

Streams can transport data between two operators in a one-to-one (or forwarding) pattern, or in a redistributing pattern. One-to-one streams preserves partitioning and order of elements, while redistributing streams change the partitioning of streams. Each operator subtask sends data to different target subtasks, depending on the selected transformation. By default each operator preserves the partitioning and order of the operator before it, thus preserving the source parallelism. While keying operations causes data reshuffling and distribution overhead, data forwarding may cause a load imbalance and even idling of cores that are not in use, thus not fully leveraging computation power of the entire cluster as shown in Figure III. Therefore, in order to guarantee efficient execution of queries, one must find the right balance between data redistribution and data forwarding. Furthermore, as parallel instances of operators cannot communicate with each other, data locality per instance must be ensured by the user.

As intelligent grouping/keying of data is application or data specific, for the effective grouping of spatial data in this work, a grid-index based data grouping and distribution is proposed. Using this distribution, all the spatial objects belonging to a particular grid cell is assigned the same key and hence is directed to the same operator’s instance. This ensures that the spatially close objects are being processed by the same operator instance and hence enables effective pruning and spatial query processing as discussed in Section VII.

IV. GEOFLINK ARCHITECTURE

Figure 2 shows the proposed GeoFlink architecture. Users can register queries to the GeoFlink system through a Scala/Java API. The API allows the users to use Java or Scala programming languages to write custom spatial queries. In order to execute Spatial Range, Spatial kNN or Spatial Join queries on the incoming data streams, a stream need to be translated into spatial data stream. Users can do so by calling the respective operation of the spatial library. At the time of writing this paper, GeoFlink supports only point spatial object, however we are working on its extension for other spatial objects including line and polygon. The query output is available to the end user via a variety of sinks including Apache Kafka, files, sockets and external systems. The GeoFlink architecture has two important layers, i.e., 1) Spatial Stream Layer and 2) Real-time Spatial Query Processing Layer.

A. Spatial Stream Layer

This layer is responsible for converting the incoming data stream(s) into spatial data stream(s). Apache Flink treats incoming data stream as ordinary text stream and its direct processing by Flink can be inefficient. GeoFlink converts the incoming data stream into spatial data stream by keeping in view the geometrical properties of spatial objects, i.e., point object, line object, polygon object, etc. This layer assigns cell ID(s) to spatial objects based on Grid-based index (refer Sec. V) for the efficient distribution and processing of incoming data stream.

B. Real-time Spatial Query Processing Layer

This layer enables the execution of spatial queries over spatial data streams. GeoFlink currently supports the most widely used spatial query operators, i.e., spatial range, spatial kNN and spatial join. The users can use Java or Scala programming languages (Scala/Java API) to write custom spatial queries. This layer makes extensive use of the grid-based index for the efficient processing of spatial queries by pruning the objects which cannot be part of the query output and by uniformly distributing data across the distributed operator instances. The query output is available to the end user via a variety of sinks including Apache Kafka, files, sockets and external systems.

V. GEOFLINK GRID INDEX

The index structures for the spatial data can be classified into broad categories, i.e., 1) Tree-based, and 2) Grid-based. The tree-based index structures supports efficient query processing, however its update cost is high, as in the case of node

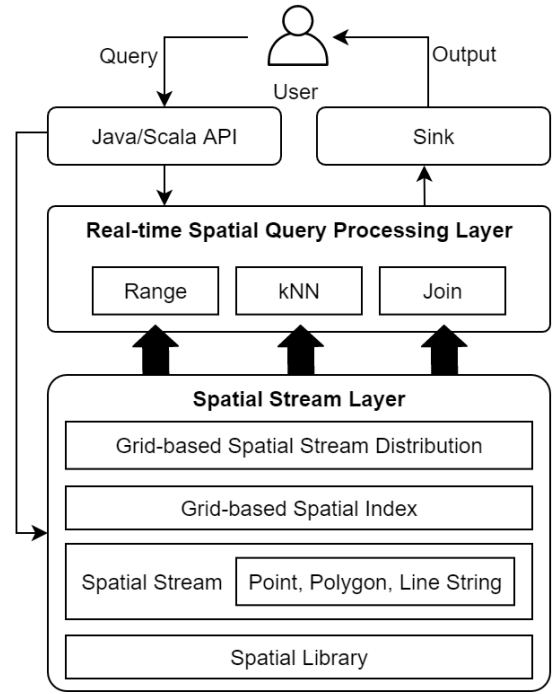


Fig. 2. GeoFlink architecture

addition, removal or update, the tree needs to be rebalanced and sometimes the whole tree needs to be restructured. On the other hand, a simple structure of grid-based index enables quick updates, however it cannot answer queries as efficiently as the tree-based index [21] [22].

Since GeoFlink is meant to support streaming applications with very high update rates, the maintenance cost of the index employed has to be as small as possible. To this end, grid-based index seems to be a natural choice for GeoFlink.

A grid-based index [23] is a space-partitioned structure where a predefined area is divided into equal-sized cells of some fixed length l , as shown in Figure 3. Geometrical objects with coordinates within the boundaries of the grid cell(s) belong to that particular cell(s). Each grid cell is identified by a unique key or ID and all the objects whose coordinates lie within the boundaries of the grid cell c is assigned the same cell key.

The grid index used in this work is aimed at pruning unnecessary objects during spatial queries execution and to help in the uniform distribution of spatial objects across the distributed cluster nodes. The grid index (G) is constructed by partitioning the 2D space given by its boundary $(MinX, MinY), (MaxX, MaxY)$ into square shaped cells of length l . Here we assume that G boundary is known as it can be estimated easily based on the geographical location of the data stream.

Let $C_{x,y} \in G$ be a grid cell with x and y indices x and y , respectively, then $L_1(C_{x,y}), L_2(C_{x,y}), \dots, L_n(C_{x,y})$ denote its neighbouring layers, where $L_1(C_{x,y})$ is given by:

$$L_1(C_{x,y}) = \{C_{u,v} | u = x \pm 1, v = y \pm 1, C_{u,v} \neq C_{x,y}\}$$

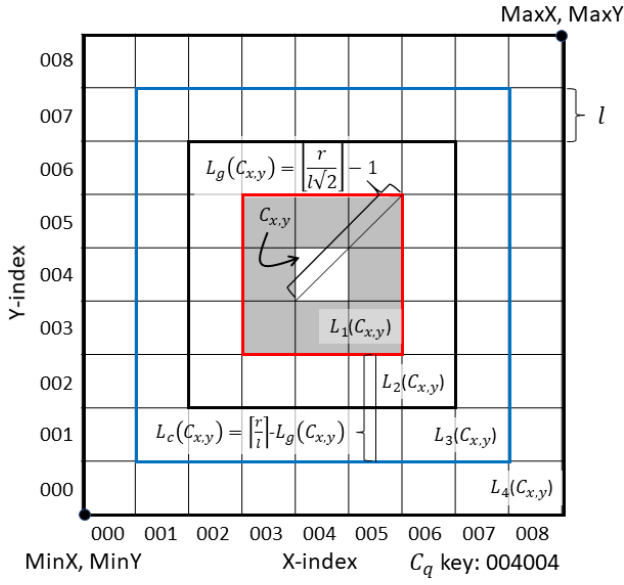


Fig. 3. GeoFlink grid index

$L_2(C_{x,y}), \dots, L_n(C_{x,y})$ are defined in a similar way. Each cell $C_{x,y} \in G$ is identified with its unique key obtained by concatenating its x and y indices. Figure 3 shows a grid structure with a cell $C_{x,y}$, its unique key, and its layers $L_1(C_{x,y}), L_2(C_{x,y}), \dots, L_n(C_{x,y})$.

Within GeoFlink, each stream tuple is assigned grid cell key(s) on its arrival, depending upon the grid cell(s) it belongs to. In this work we assume that a point geometrical object can only belong to a single cell, whereas the geometrical objects: lines and polygons, can belong to multiple cells depending upon its size and position. Hence, a single cell key is assigned to a point whereas an array of key(s) need to be assigned to lines and polygons. In this work our focus is only point object, hence one grid cell key is assigned per stream tuple. Let S denotes a spatial stream then the coordinates of the tuples $s \in S$ are given by $s.x$ and $s.y$. Given grid G and its boundary $(MinX, MinY), (MaxX, MaxY)$, a stream tuple key is computed as follows:

$$xIndex = \frac{\lfloor s.x - G.MinX \rfloor}{l}$$

$$yIndex = \frac{\lfloor s.y - G.MinY \rfloor}{l}$$

$$s.key = xIndex \odot yIndex$$

where $xIndex$ and $yIndex$ are fixed length (n) indices and \odot denotes the concatenation operator.

For instance, a grid G is given by a boundary $(MinX, MinY), (MaxX, MaxY) = (0, 0), (50, 50)$. For a stream tuple s with coordinates $(25, 42)$ and $n = 3$, its key s given by: $xIndex = 2 = 002$, $yIndex = 4 = 004$, $s.key = 002004$.

The grid-based index used in this work is logical, that is, it only assigns a key (cell ID) to incoming streaming tuples or

moving objects and based on the key, the tuples are processed, pruned and distributed across the cluster nodes. Beside the assignment of a key to streaming tuples, no physical data structure is needed, hence no update is required when a stream tuple expires or an updated object location is received. This makes our grid-based index fast and memory efficient.

VI. SPATIAL STREAM LAYER

Spatial streams in GeoFlink are distributed streams where each tuple represents a spatial object. For the effective distribution of data streams that take into account the spatial proximity of data so to speed up spatial query processing across the GeoFlink cluster nodes, grid-based index (V) is used.

A. Spatial Stream Indexing

Spatial indexes like R-tree, Quad-tree and KDB-tree can significantly speed-up spatial query processing, however their maintenance cost is high especially in the presence of heavy insertions and deletions [24] [25] [26].

Since GeoFlink is meant to support streaming applications with very high update rates, tree-based index is not a good choice. Instead we need a spatial index which can support efficient query processing and uniform data distribution across the distributed cluster nodes. Therefore, GeoFlink uses a very light and update-efficient grid based index as discussed in Section V.

One problem with the grid-based index is that it requires data boundaries for its construction. Since a stream is dynamic and infinite, its boundaries cannot be known in advance however, it can be easily estimated based on the geographical location of the sensors generating the data streams in case of fixed sensors or if the data stream is being generated by moving objects, it can be estimated by utilizing the loose bounds of the area or city of the objects. For instance, assuming that we are aware of the city of the data stream source(s), we can use the city's geographical boundaries for the grid-index creation. A GeoFlink Java API example of constructing the grid-based index is given below.

```
UniformGrid uGrid = new UniformGrid
(GridSize, MinX, MaxX, MinY, MaxY)
```

where *GridSize* of 50 generates a grid index of 50x50 cells, with the bottom-left (MinX, MinY) and top-right (MaxX, MaxY) coordinates, respectively.

B. Spatial Objects Support

GeoFlink currently supports *CSV* and *GeoJSON* input formats from Apache Kafka and *Point* type spatial object, however we are working on its extension to support other input formats and spatial object types including line and polygon.

GeoFlink users need to make an appropriate Apache Kafka connection by specifying the topic name and bootstrap server(s). Once the connection is established, the user can construct spatial stream using the GeoFlink Java/Scala API. A GeoFlink Java API example of constructing a spatial stream from GeoJSON stream is as follows.

```
// GeoJSON input stream
DataStream<Point> pointStream = SpatialStream.
PointStream(geoJSONStream, "GeoJSON", gridIndex);
```

C. Spatial Stream Partitioning

Effective partitioning of data across distributed cluster nodes plays a vital role in efficient query processing. As discussed in Section III, Apache Flink *keyBy* transformation logically partitions a stream into disjoint partitions in such a way that all the tuples with the same key are assigned to the same partition or to the same operator instance. Internally, the *keyBy* transformation is implemented using hash partitioning.

To enable effective partitioning in GeoFlink, which takes into account the incoming data's spatial proximity, grid indexing is used. GeoFlink assigns a grid cell ID (*key*) to each incoming stream tuple based on its spatial location. Since all spatially close tuples belong to a single grid cell, they are assigned the same *key*. GeoFlink uses the *key* as the *keyBy* operator's key to enable effective stream distribution across the distributed operator instances. The grid index creation is discussed in Section VI-A, whereas the *key* assignment is done as part of the spatial objects creation as discussed in Section VI-B. Stream partitioning is further discussed in Section VII.

VII. REAL-TIME SPATIAL QUERY PROCESSING LAYER

The real-time spatial query processing layer of GeoFlink provides support for all the basic spatial operators which are required by any spatial data processing and analysis applications. The supported queries/operators include spatial range query, spatial *k*NN query and spatial join query. All the queries discussed in this section make use of aggregation window and are continuous in nature, i.e., they generate window-based continuous results on the continuous data stream. Namely, one output is generated per window aggregation.

To reduce spatial query execution cost and to distribute the spatial data effectively across the cluster nodes, GeoFlink makes use of the grid index structure. One traditional and a very effective way to reduce the computation cost is to prune out the objects which cannot be part of the query result. Given a cell $C_{x,y} \in G$ containing a query object, we define the following layers for the sake of effective pruning, where a layer is made up of grid cells as discussed in Section V.

- **Guaranteed Layers** ($L_g(C_{x,y})$): The objects in this layer are guaranteed to be part of the query result.
- **Candidate Layers** ($L_c(C_{x,y})$): The objects in this layer may or may not be the part of the query result and hence require (distance) evaluation.
- **Non-neighbouring Layers** ($L_n(C_{x,y})$): The objects in this layer cannot be part of the query result and hence can be safely pruned

The cells in the layers $L_g(C_{x,y})$, $L_c(C_{x,y})$ and $L_n(C_{x,y})$ are disjoint. In the following, we call the objects belonging to the $L_g(C_{x,y})$, $L_c(C_{x,y})$ and $L_n(C_{x,y})$ layers as the guaranteed neighbours, candidate neighbours and non-neighbours, respectively. Since most of the spatial queries deal with the

neighbourhood computation, we define *r*-neighbours of a query point *q* as follows.

Definition 1 (r-neighbours(q)): Geometrical objects that lie within the radius *r* of *q*.

Let *l*, *q* and *r* denotes a grid cell length, a query point and the query radius, respectively. Assuming that a cell $C_{x,y}$ contains a query point *q* as shown in Figure 3, then the layers $L_g(C_{x,y})$ and $L_c(C_{x,y})$ are given as follows:

$$L_g(C_{x,y}) = \lfloor \frac{r}{l\sqrt{2}} \rfloor - 1 \quad (1)$$

$$L_c(C_{x,y}) = \lceil \frac{r}{l} \rceil - L_g(C_{x,y}) \quad (2)$$

The layers other than $L_g(C_{x,y})$ and $L_c(C_{x,y})$ are the *non-neighbouring layers*, i.e., $L_n(C_{x,y})$.

A. Spatial Range Query

Definition 2 (Spatial Range Query): Given a data stream *S*, query point *q*, radius *r* and window parameters, range query returns the *r*-neighbours of *q* in *S* for each aggregation window.

A spatial range query returns all the spatial objects in the spatial stream *S*, that lie within the *r*-distance of the query point. The query results are generated periodically, based on the window size. Such a query can be easily distributed and parallelized, i.e., the incoming stream can be divided across the cluster nodes, where each tuple is checked for the *r*-neighbours(*q*). This approach require computing the distance between all the incoming objects and the query object, which can be computationally expensive especially when the distance computation is expensive, for instance, road distance.

A more efficient way is to filter out the objects which cannot be part of the query result and thus reduce the number of distance computations and the query cost. Hence, we propose a grid-based spatial range query consisting of *Filter* and *Refine* phases, where the *Filter* phase eliminates objects which cannot be part of the query output and the *Refine* phase evaluates the unpruned objects using the distance function.

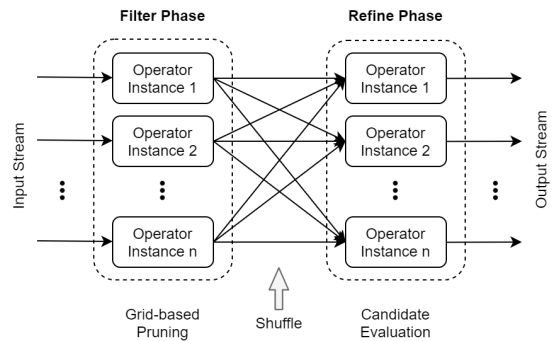


Fig. 4. Spatial Range Query Data Flow

Algorithm 1 and Figure 7 details the different phases of the grid-based range query. GeoFlink receives data streams from a distributed messaging system, for instance, Apache Kafka

Algorithm 1 Spatial Range Query

Input: S_{in} : Spatial data stream, q : query object, r : Query radius, G : Spatial grid index

Output: S_{out} : Spatial stream containing objects that satisfy the range query predicate

- 1: Get C_q using $q.key$; $\{C_q$ denotes the cell containing $q\}$
 - 2: Compute $L_g(C_q)$ and $L_c(C_q)$ using Equations 1 and 2, respectively.
{Filter Phase}
 - 3: **for each** $s \in S_{in}$ **do**
 - 4: **if** $s \in L_g(C_q)$ **then**
 - 5: s is a guaranteed r -neighbour(q) and is added to S_{out}
 - 6: **else if** $s \in L_c(C_q)$ **then**
 - 7: s is a candidate neighbour and is added to S_{candid}
 - 8: **end if**
 - 9: **end for**
 - 10: Shuffle S_{candid} to balance the load across cluster nodes
{Refine Phase}
 - 11: **for each** $s \in S_{candid}$ **do**
 - 12: **if** $s \in r$ -neighbour(q) **then**
 - 13: Add s to S_{out} $\{s \in r$ -neighbour(q) is computed using distance function}
 - 14: **end if**
 - 15: Return S_{out}
 - 16: **end for**
-

[27]. Provided the right configuration, the binding between stream source cluster and Apache Flink cluster enables the uniform distribution of incoming stream across the Flink cluster nodes. Given the query point q , each GeoFlink node computes the $L_g(C_q)$ and $L_c(C_q)$ sets, where C_q denotes the cell containing q . The algorithm 1 consists of two main phases, i.e., the filter phase and the refine phase. The filter phase prunes out the input spatial stream (S_{in}) tuples which are not part of $L_g(C_q)$ or $L_c(q)$. As a result of filtering, majority of tuples are pruned out, while a few are sent to the output stream (S_{out}) and the remaining candidate neighbours (S_{candid}) require refine phase. After the filter phase, a small shuffling is done to rebalance the data stream. Finally in the refine phase, S_{candid} are checked for the r -neighbour(q) using the actual distance function.

To execute a spatial range query via GeoFlink Java/Scala API *SpatialRangeQuery* method of the *RangeQuery* class is used. We first create a query point and then pass it to the *SpatialRangeQuery* method along with the spatial data stream and other required parameters.

```
// Create a query point q
Point queryPoint = new Point (qLongitude ,
qLatitude , uGrid);

// Register a spatial range query
DataStream<Point> outputStream = RangeQuery.
SpatialRangeQuery (pointStream , queryPoint ,
radius , windowSize , windowSlideStep , uGrid);
```

where *pointStream* is a spatial point data stream,

queryPoint denotes a query point, *radius* denotes the range query radius, *windowSize* and *windowSlideStep* denote the sliding window query size and slide step respectively. The query output is generated continuously for each window slide based on the *windowSize* and *windowSlideStep*.

B. Spatial k NN Query

Definition 3 (Spatial k NN Query): Given a data stream S , a query point q , a positive integer k and window parameters, k NN query returns k nearest neighbours of q in S for each aggregation window.

The spatial k NN query returns the window-based k nearest neighbours of q in the spatial stream S . The query ranks the distances between the spatial objects and the query object q and returns the k nearest neighbours periodically based on window size. Just like the spatial range query, this query can be easily distributed and parallelized, i.e., the incoming stream tuples can be divided across the cluster nodes, where each node computes and maintains its k nearest neighbours. The k NN are then merged and sorted at a single cluster node to generate the true k NNs per window. This approach requires computing the distance between all the incoming objects and the query object.

A more efficient way is to filter out the objects which cannot be part of the query result and thus reduce the number of distance computations and the query cost. This work proposes a grid-based k NN query consisting of the *Filter*, *Refine* and *Sorting* phases as shown in Figure 8, where in the *Filter* phase, the objects which cannot be part of the query output are pruned out, in the *Refine* phase, distance function based computation is done for the unpruned objects and the *Sorting* phase is responsible for merging and sorting the k NNs from the distributed GeoFlink cluster nodes.

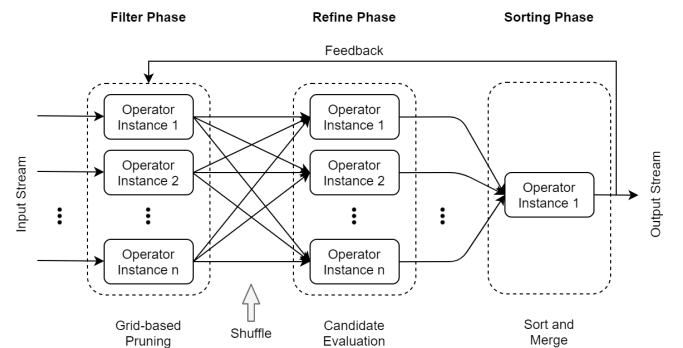


Fig. 5. k NN Query Data Flow

Algorithm 2 details the different phases of the grid-based k NN query. In contrast to the range query (Sec. VII-A), there is no query radius available in advance for the k NN query, hence the pruning layers $L_g(C_q)$ and $L_c(C_q)$ cannot be computed directly. To enable the pruning of non- k NN neighbours for the effective k NN computation we made use of feedback/iterative approach.

For the first iteration (window), the algorithm computes the k NNs using all the spatial stream tuples, which is similar to

that of the naive approach. However, after the first iteration, the distance of the k^{th} nearest neighbour from q , d_k , is sent back to the filter phase. The filter phase uses the d_k to estimate the candidate neighbouring layers $L_c(q)$ in the next iteration and hence can prune the non-neighbouring objects in the non-neighbouring layers $L_n(q)$. To maximize the chances of obtaining at least k NN from every window/iteration, the d_k is multiplied with a constant factor α , where $\alpha > 1$. The execution continues in a similar fashion, with the feedback being sent back after every iteration and thus enabling the updates of the $L_c(q)$ and $L_n(q)$ continuously.

Algorithm 2 Spatial k NN Query

Input: S_{in} : Spatial data stream, q : query object, k : number of nearest neighbours required, α : Multiplication factor, G : Spatial grid index
Output: S_{out} : Spatial stream containing the k NN objects with respect to q

- 1: $L_c(C_q) = m$ { m : Max. number of grid layers}
 {Filter Phase}
- 2: **for each** $s \in S_{in}$ **do**
- 3: **if** $s \in L_c(q)$ **then**
- 4: s is a candidate neighbour and is added to S_{candid}
- 5: **end if**
- 6: **end for**
- 7: Shuffle S_{candid} to balance the load across the cluster nodes
 {Refine Phase}
- 8: **for each** $s \in S_{candid}$ **do**
- 9: **if** s is a k NN **then**
- 10: Add s to S_{pre_out}
- 11: **end if**
- 12: **end for**
 {Sorting Phase}
- 13: Merge and sort k NNs (S_{pre_out}) from all the cluster nodes to obtain the combined k NN and add the results to the S_{out}
- 14: $d_k = dist(q, k^{th}NN)$ { $k^{th}NN$ denotes the k^{th} nearest neighbour}
- 15: Update $L_c(C_q)$ using $k^{th}NN$ for the next iteration and send it back to the Filter Phase; $L_c(C_q) = \lceil \frac{\alpha * d_k}{t} \rceil$;
- 16: Return S_{out}

To execute a spatial k NN query via the GeoFlink Java/Scala API *SpatialKNNQuery* method of the *KNNQuery* class is used.

```
// Create a query point q
Point queryPoint = new Point (qLongitude ,
qLatitude , uGrid);

// Register a spatial kNN query
DataStream <PriorityQueue<Tuple2<Point ,
Double>>> outputStream = KNNQuery.
SpatialKNNQuery(spatialStream , queryPoint ,
k , windowSize , windowSlideStep , uGrid);
```

where k denotes the number of points required in the k NN output. Please note that the output stream is a stream of priority queue which is a sorted list of k NNs with respect to the

distance from the query point q . The query output is generated continuously for each window slide based on the *windowSize* and *windowSlideStep*.

Algorithm 3 Spatial Join Query

Input: $S1$: Spatial ordinary data stream, $S2$: Spatial query data stream, q : query object, r : Query radius, G : Spatial grid index
Output: S_{out} : Joined spatial stream
 {Replication Phase}

- 1: **for each** $q \in S2$ **do**
- 2: Get C_q using $q.key$; { C_q denotes the cell containing q }
- 3: Compute $L_g(C_q)$ and $L_c(C_q)$ using Equations 1 and 2, respectively.
- 4: $S2' = \text{Replicate } S2$, such that each $q \in S2$ is assigned keys from the sets $L_g(C_q)$ and $L_c(C_q)$;
- 5: **end for**
- 6: Distribute $S1$ and $S2'$ across the cluster nodes based on their keys
 {Filter Phase}
- 7: **for each** $q \in S2'$ **do**
- 8: **for each** $s \in S1$ **do**
- 9: **if** s lies in $L_g(C_q)$ **then**
- 10: s is a guaranteed neighbour and is added to S_{out}
- 11: **else if** $s \in L_c(C_q)$ **then**
- 12: s is a candidate neighbour and is added to S_{candid}
- 13: **end if**
- 14: **end for**
- 15: **end for**
 {Refine Phase}
- 16: **for each** $q \in S2'$ **do**
- 17: **for each** $s \in S_{candid}$ **do**
- 18: **if** $s \in r$ -neighbour(q) **then**
- 19: Add s to S_{out}
- 20: **end if**
- 21: **end for**
- 22: **end for**
- 23: Return S_{out}

C. Spatial Join Query

Spatial join is an expensive operation, where each tuple of a query stream must be checked against every tuple of an ordinary stream. To achieve this using the naive approach, low rate stream (query stream) is replicated across all the cluster nodes whereas the high rate stream (ordinary stream) is divided across the cluster nodes. However, this involves expensive distance computations and heavy shuffling of stream tuples. Definition 4 formally defines the spatial join.

Definition 4: [Spatial Join Query] Given two streams $S1$ (ordinary stream) and $S2$ (query stream), a radius r and window parameters, spatial join query returns all the points in $S1$ that lie within the radius r of $S2$ points for each aggregation window.

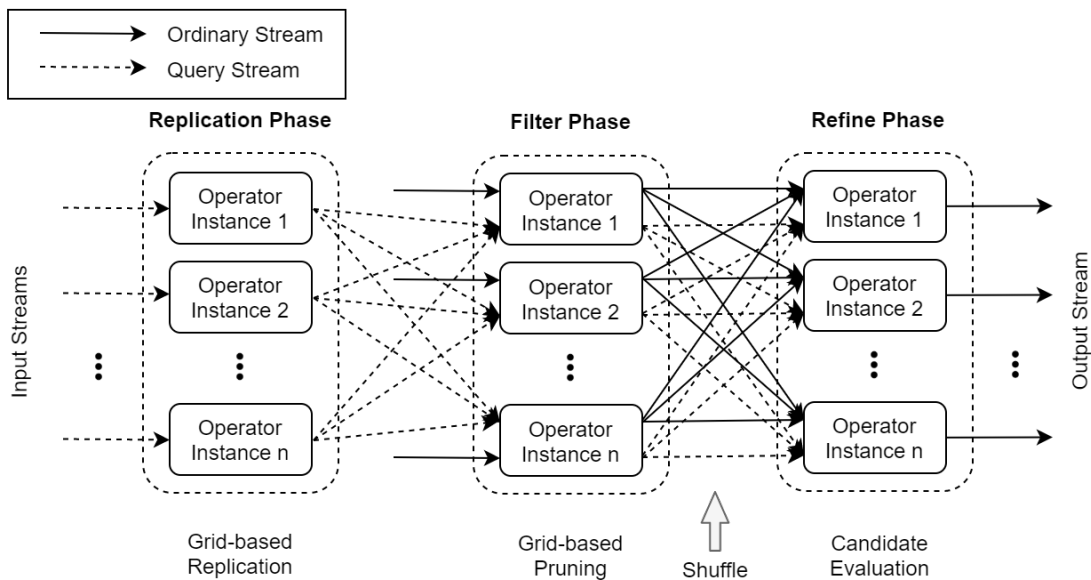


Fig. 6. Spatial Join Query Data Flow

To reduce the number of distance computations by pruning ordinary stream tuples which cannot be part of the query result and to reduce data shuffling, we made use of grid index. Since the grid index takes into account the spatial proximity of spatial objects, a number of objects can be filtered out resulting in efficient join processing.

Figure 6 gives an overview of the GeoFlink spatial join. The grid-based spatial join consists of the following three phases: 1) Replication phase, 2) Filter phase, and 3) Refine phase. Let S_1 and S_2 denote the ordinary stream and the query stream, respectively. Given the spatial join query radius r , the replication phase computes the $L_g(C_q)$ and $L_c(C_q)$ of each $C_q | q \in S_2$, where C_q denotes the cell containing query q . Next, the query points are replicated in such a way that each replicated point is assigned a cell ID (key) from the set $L_c(C_q)$. We denote the replicated query stream by S_2' . Next, we make use of the Apache Flink's key-based join to join the two stream. Flink's key-based join enables the tuples from the two joining streams with the same key to land on the same operator instance, hence enabling effective joining by filtering out the tuples which cannot be part of the join result. Hence, we join S_1 with S_2' on keys. This causes the join to be executed only between the query point $q \in S_1$ and the ordinary stream points which belong to the cells in $L_c(C_q)$ in the refine phase. The S_1 objects which belong to the cells in $L_g(C_q)$ are guaranteed to be part of the join output and hence can be added to the output stream. Algorithm 3 lists the main steps of the spatial join query.

To execute a spatial join query via the GeoFlink Java/Scala API `SpatialJoinQuery` method of the `JoinQuery` class is used. The query output is generated continuously for each window slide based on the `windowSize` and `windowSlideStep`.

```
// Create a query stream
DataStream<Point> queryStream = SpatialStream .
```

```
PointStream ( geoJSONQryStream , "GeoJSON" , uGrid );
```

```
// Register a spatial join query
DataStream<Tuple2<String , String >>outputStream=
JoinQuery . SpatialJoinQuery ( spatialStream ,
queryStream , radius , windowSize , windowSlideStep ,
uGrid );
```

VIII. EXPERIMENTAL EVALUATION

This section presents the detailed experimental evaluation of GeoFlink. In particular, we evaluated the throughput of GeoFlink for the three spatial queries, i.e., Spatial Range, Spatial kNN and Spatial Join.

A. Data streams

For performance evaluation of GeoFlink, a real dataset, Microsoft T-Drive trajectory data [28], containing GPS trajectories of 10,357 taxis during the period of February 2 to 8, 2008 in Beijing city is used. The total number of points (tuples) in the dataset is 17 million and the total distance of the trajectories is around 9 million kilometres. Each tuple consists of a taxi ID, datetime, longitude and latitude. The dataset is loaded into the Apache Kafka [27] system and is supplied as a distributed data stream to the GeoFlink cluster.

B. Environment

For the experiments, Apache Kafka and Apache Flink clusters are used. The clusters are deployed on AIST AAIC cloud [29], where each VM has 128 GB memory and 20 CPU cores and each core uses Intel skylake 1800 MHz processor. Table I shows the deployment details of each cluster. All the VMs are operated using Ubuntu 16.04 LTS.

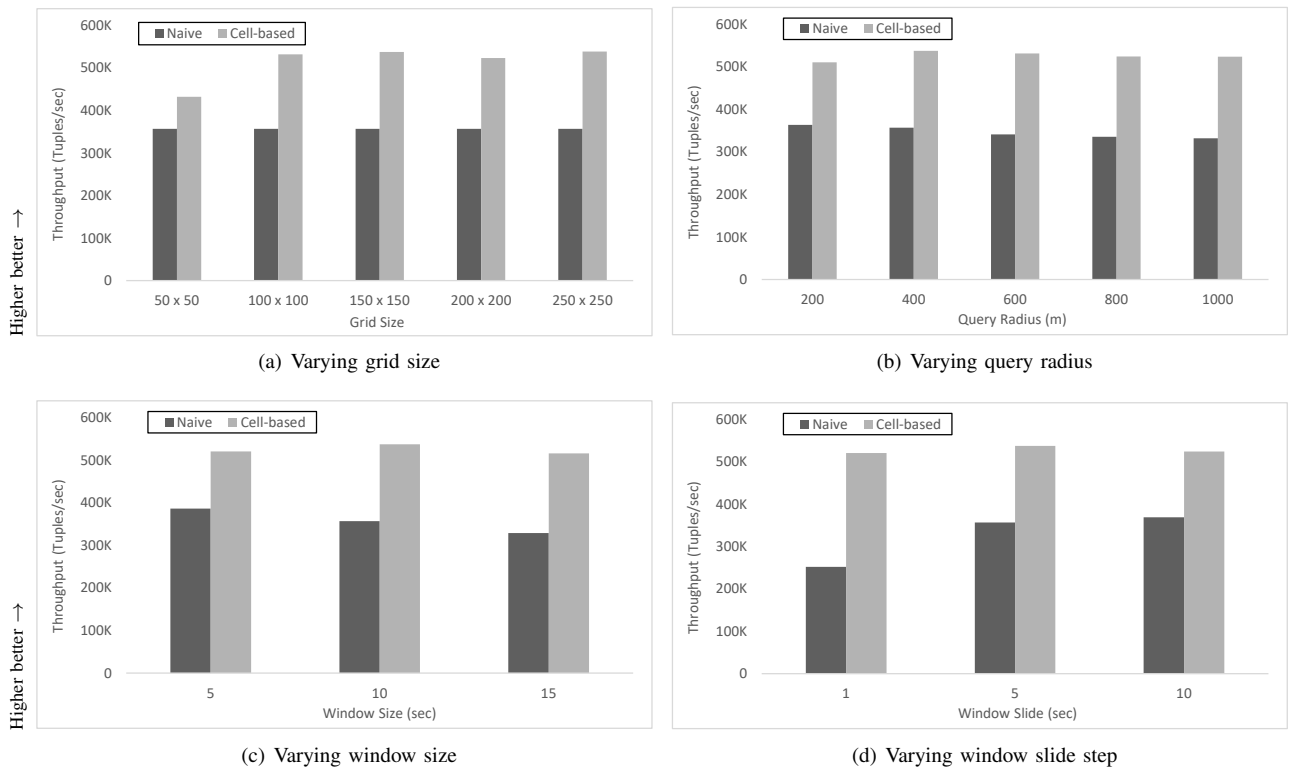


Fig. 7. Spatial range query

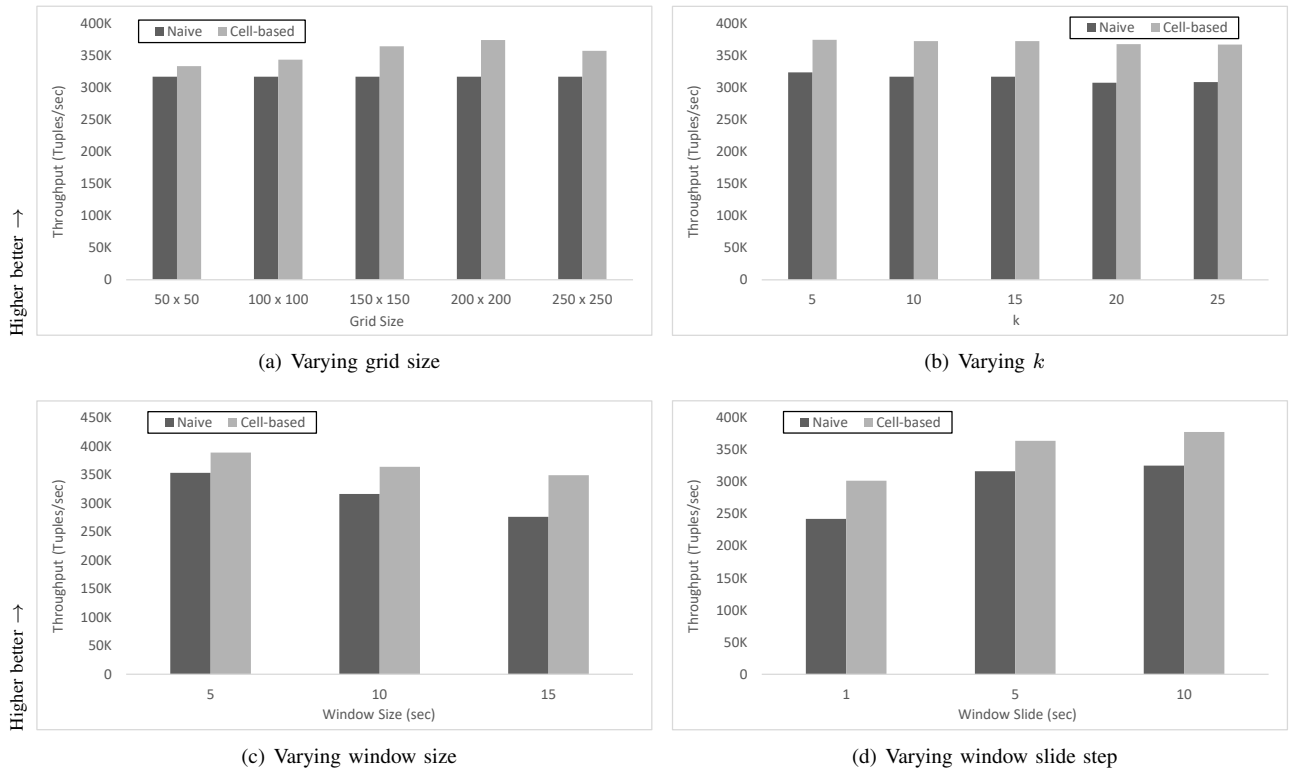


Fig. 8. Spatial kNN query

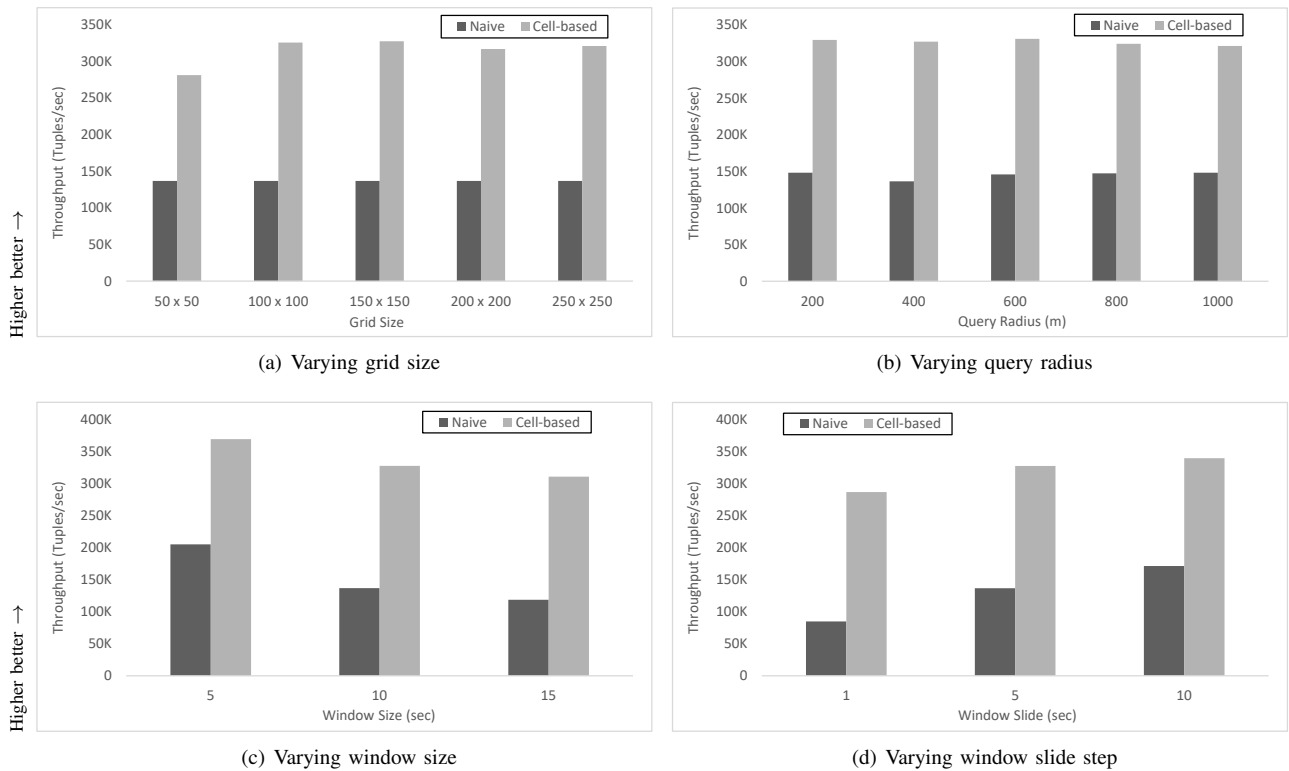


Fig. 9. Spatial join query

TABLE I
DEPLOYMENT DETAILS OF EXPERIMENTATION CLUSTERS

Cluster	# Nodes	Memory	Version
Apache Flink	4 ^a	128 GB	1.9.1
Apache Kafka	3 ^b	128 GB	2.3.0

^a 1 Job Manager and 3 Task Managers

^b 1 Zookeeper and 2 Broker Nodes

C. Evaluation

The section presents the evaluation results of the three queries discussed in Section VII. We compared the grid-based implementation of GeoFlink queries with the respective naive approaches, which are discussed in Section VII. For fair comparison, efforts are made to distribute the data stream uniformly across the cluster nodes however the respective naive approaches lack the grid-based pruning. The evaluation is presented in terms of the system throughput, which can be defined as the maximum number of stream tuples which can be processed by the system per second. Unless otherwise stated, following default parameter values are used in the experiments: grid size: 150 x 150 cells, query radius r : 400 meters, window size: 10 seconds, window slide: 5 seconds and k : 10. Each experiment is performed three times and the average values are reported in the graphs. To construct the grid, the end-user needs to provide the approximate/loose boundaries of the data stream. For instance, in the case of

the T-Drive data stream in this work we made use of the following rectangular boundary in terms of longitudes and latitudes, which covers Beijing city: bottom-left = 115.50000, 39.60000, top-right = 117.60000, 41.10000. Simple Euclidean distance is used for the distance computation.

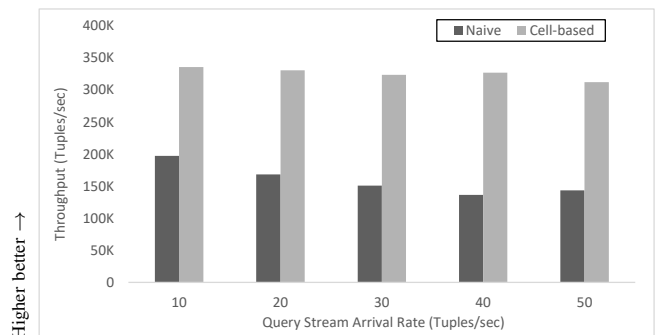


Fig. 10. Join query: varying query stream arrival rate

Figure 7 compares system throughput of our cell-based approach with the naive approach for the spatial range query by varying different parameters. The system throughput of the cell-based approach is far higher compared to the naive approach for all the variation of the parameters, which is mainly due to the effective grid-based pruning. In Figure 7(a), throughput of the cell-based approach is comparatively lower for the grid size 50 x 50. This is because at this grid size, each individual cell size is quite large, hence resulting in poor

pruning. On the other hand very small cell sizes also result in lower throughput as can be observed from the grid sizes 200 x 200 and 250 x 250, which is due to the fact that the small cell sizes increases the number of cells exponentially, whose processing incurs higher processing cost hence reducing the system throughput. In Figure 7(b) we varied the query radius. Since the increase in query radius results in bigger query evaluation set, the throughput decreases with the increase in the query radius, however the decrease is significant in the naive approach compared to the cell-based approach. This is again due to the strong pruning capability of the cell-based approach. In Figures 7(c) and 7(d), the window size and slide step are varied. Increasing window size results in a decrease in the throughput which is quite obvious however, again the decrease is less significant in the cell-based approach proving the effectiveness of the grid-based approach. On the other hand, increasing the window slide step in Figure 7(d) results in an increase in the system throughput, because larger slide step means less overlapping computation as the window slides. This results in the decrease in the number of distance computations and hence increase in the system throughput.

In Figure 8 we evaluated the k NN query by varying different parameters. For the cell-based k NN evaluation, the α value is set to 1.5. Although the throughput of the cell-based approach is comparatively better than the naive approach in all cases, the difference is not significant. This is due to the fact that the k NN cell-based approach utilizes a feedback approach rather than direct pruning as in the case of the range query. Hence, pruning is not as good as in the case of the range query. Furthermore, implementation of the iterative/feedback approach incurs an additional operator in the cell-based approach resulting in the reduced throughput. The variation of parameters has more or less the same effect on the processing of the k NN query as in the case of the range query. The only new parameter in the k NN query is k , in Figure 8(b). Increasing the parameter k decreases the system throughput because for the larger k values, the system needs to maintain bigger priority queues to keep the k NN sorted. Since the proposed grid-based k NN can prune a large number of objects and require far less distance computations compared to the naive approach, our approach will be more beneficial when expensive distance computations are used, for instance, the road distance computation.

Figure 9 evaluates the spatial join query by varying different parameters. From the figure, the throughput of the cell-based join query is comparatively far higher than the naive approach, and in most cases more than the double. This is because the join query involves multiple query points, which means that the naive approach now needs to deal with a large number of points and distance computations. However, in case of the grid-based approach, majority of the non-neighbours can be pruned out and the join query requires far less number of distance computations. The trends in the variation of the parameters including grid size, query radius, window size and window join are essentially the same as that of the previous queries. The Figure 9 includes variation in the query stream arrival

rate as an additional evaluation. The increase in the query stream arrival rate results in the reduced system throughput, which is obvious as with the increase in the number of query points, more computations are needed. However, this reduction is quite significant in the naive approach compared to the cell-based approach, proving the effectiveness of the cell-based approach.

IX. CONCLUSION AND FUTURE WORK

This work presents GeoFlink which extends Apache Flink to support spatial data types, index and continuous queries. To enable the efficient processing of continuous spatial queries and the effective data distribution among the Flink cluster nodes, a grid-based index is introduced. The grid index enables the pruning of spatial objects which cannot be part of a spatial query result and thus can guarantee efficient query processing, similarly it helps in preserving the spatial data proximity resulting in effective data distribution.

GeoFlink currently supports spatial range, spatial k NN and spatial join queries on geometrical point data type. Extensive experimental study proves that GeoFlink's grid-based approach can significantly improve the system throughput by pruning a large number of data points. As a future direction, we are working on GeoFlink's extension to support line and polygon data types and other complex query operators.

REFERENCES

- [1] PostGIS, "PostGIS: Spatial and Geographic objects for PostgreSQL," <http://postgis.net/>, [Online; accessed 10-March-2020].
- [2] QGIS, "Qgis, a free and open source geographic information system," <https://qgis.org/en/site/>, 2020, [Online; accessed 31-March-2020].
- [3] T. A. S. Foundation., "Apache Spark - Lightning-Fast Cluster Computing," <http://spark.apache.org/>, [Online; accessed 11-November-2018].
- [4] A. Flink, "Flink cep," <https://ci.apache.org/projects/flink/flink-docs-stable/dev/libs/cep.html>, 2019, [Online; accessed 01-August-2019].
- [5] T. A. S. Foundation, "Apache Samza - Distributed Stream Processing," <http://samza.apache.org/>, [Online; accessed 11-November-2018].
- [6] A. Storm, "Apache Storm: Distributed realtime computation system," <https://storm.apache.org/>, [Online; accessed 10-March-2020].
- [7] A. Aji, F. Wang, H. Vo, R. Lee, Q. Liu, X. Zhang, and J. Saltz, "Hadoop gis: A high performance spatial data warehousing system over mapreduce," *Proc. VLDB Endow.*, vol. 6, no. 11, p. 10091020, Aug. 2013. [Online]. Available: <https://doi.org/10.14778/2536222.2536227>
- [8] A. Eldawy and M. F. Mokbel, "Spatialhadoop: A mapreduce framework for spatial data," in *2015 IEEE 31st International Conference on Data Engineering*, April 2015, pp. 1352–1363.
- [9] J. Yu, Z. Zhang, and M. Sarwat, "Spatial data management in apache spark: the geospatial perspective and beyond," *GeoInformatica*, vol. 23, no. 1, pp. 37–78, 2019. [Online]. Available: <https://doi.org/10.1007/s10707-018-0330-9>
- [10] J. Lu and R. Gting, "Parallel secondo: Boosting database engines with hadoop," 12 2012, pp. 738–743.
- [11] J. N. Hughes, A. Annex, C. N. Eichelberger, A. Fox, A. Hulbert, and M. Ronquest, "GeoMesa: a distributed architecture for spatio-temporal fusion," in *Geospatial Informatics, Fusion, and Motion Video Analytics V*, M. F. Pallechia, K. Palaniappan, P. J. Doucette, S. L. Dockstader, G. Seetharaman, and P. B. Deignan, Eds., vol. 9473, International Society for Optics and Photonics. SPIE, 2015, pp. 128 – 140.
- [12] D. Sidlauskas, S. Saltenis, C. W. Christiansen, J. M. Johansen, and D. Saulys, "Trees or grids?: indexing moving objects in main memory," in *17th ACM SIGSPATIAL International Symposium on Advances in Geographic Information Systems, ACM-GIS 2009, November 4-6, 2009, Seattle, Washington, USA, Proceedings*, 2009, pp. 236–245.
- [13] ESRI, "Esri: See patterns, connections, and relationships," <https://www.esri.com/>, [Online; accessed 12-November-2019].

- [14] M. Erwig and M. Schneider, *STQL — A Spatio-Temporal Query Language*. Boston, MA: Springer US, 2002, pp. 105–126.
- [15] S. You, J. Zhang, and L. Gruenwald, “Large-scale spatial join query processing in cloud,” in *2015 31st IEEE International Conference on Data Engineering Workshops*, April 2015, pp. 34–41.
- [16] M. Tang, Y. Yu, W. G. Aref, A. R. Mahmood, Q. M. Malluhi, and M. Ouzzani, “Locationspark: In-memory distributed spatial query processing and optimization,” *ArXiv*, vol. abs/1907.03736, 2019.
- [17] F. Baig, H. Vo, T. M. Kurç, J. H. Saltz, and F. Wang, “Sparkgis: Resource aware efficient in-memory spatial query processing,” in *Proceedings of the 25th ACM SIGSPATIAL International Conference on Advances in Geographic Information Systems, GIS 2017, Redondo Beach, CA, USA, November 7-10, 2017*, E. G. Hoel, S. D. Newsam, S. Ravada, R. Tamassia, and G. Trajcevski, Eds. ACM, 2017, pp. 28:1–28:10. [Online]. Available: <https://doi.org/10.1145/3139958.3140019>
- [18] F. A. Ahmed, J. Ye, and J. Arthur, “Evaluating streaming frameworks for large-scale event streaming,” <https://medium.com/adobetech/evaluating-streaming-frameworks-for-large-scale-event-streaming-7209938373c8form>, 2019, [Online; accessed 10-March-2020].
- [19] F. Zhang, Y. Zheng, D. Xu, Z. Du, Y. Wang, R. Liu, and X. Ye, “Real-time spatial queries for moving objects using storm topology,” *ISPRS International Journal of Geo-Information*, vol. 5, no. 10, p. 178, Sep 2016.
- [20] ApacheFlinkDoc, “Dataflow Programming Model,” <https://ci.apache.org/projects/flink/flink-docs-stable/concepts/programming-model.html>, 2019, [Online; accessed 06-November-2019].
- [21] Y. Manolopoulos, Y. Theodoridis, and V. J. Tsotras, *Spatial Indexing Techniques*. Boston, MA: Springer US, 2009, pp. 2702–2707.
- [22] R. H. Guting, “An introduction to spatial database systems,” *VLDB Journal*, vol. 3, pp. 357 – 399, 1994.
- [23] J. L. Bentley and J. H. Friedman, “Data structures for range searching,” *ACM Comput. Surv.*, vol. 11, no. 4, pp. 397–409, Dec. 1979. [Online]. Available: <http://doi.acm.org/10.1145/356789.356797>
- [24] M. Hadjieleftheriou, Y. Manolopoulos, Y. Theodoridis, and V. J. Tsotras, *R-Trees: A Dynamic Index Structure for Spatial Searching*. Cham: Springer International Publishing, 2017, pp. 1805–1817.
- [25] M. L. Lee, W. Hsu, C. S. Jensen, B. Cui, and K. L. Teo, “Supporting frequent updates in r-trees: A bottom-up approach,” in *Proceedings of the 29th International Conference on Very Large Data Bases - Volume 29*, ser. VLDB 03. VLDB Endowment, 2003, p. 608619.
- [26] C. A. Shaffer and H. Samet, “Optimal quadtree construction algorithms,” *Computer Vision, Graphics, and Image Processing*, vol. 37, no. 3, pp. 402 – 419, 1987.
- [27] T. A. S. Foundation, “Apache Kafka - A Distributed Streaming Platform,” <http://spark.apache.org/>, [Online; accessed 11-November-2018].
- [28] J. Yuan, Y. Zheng, X. Xie, and G. Sun, “Driving with knowledge from the physical world,” in *Proceedings of the 17th ACM SIGKDD International Conference on Knowledge Discovery and Data Mining*, ser. KDD 11. New York, NY, USA: Association for Computing Machinery, 2011, p. 316324. [Online]. Available: <https://doi.org/10.1145/2020408.2020462>
- [29] N. I. of Advanced Industrial Science and T. (AIST), “Aist artificial intelligence cloud (aaic),” <https://www.airc.aist.go.jp>, [Online; accessed 4-April-2019].